Scholar Publishing Group
International Journal of Public Health and Preventive Medicine
https://doi.org/10.38007/IJPHPM.2020.010203
ISSN 2789-8377 Vol. 1, Issue 2: 24-40

Method for Tracking Vascular Movement of the Elderly Based on Four-Dimensional Medical Imaging

Lei Wang*

School of Design, Zhejiang Tech University, Hangzhou, Zhejiang 315100, China

wanglei@zjut.edu.cn

**corresponding author*

Keywords: Four-Dimensional Medical Imaging, Computational Intelligence for Healthcare, Blood Vessel Movement in the Elderly, Tracking Method, Four-Dimensional Vessel Modeling

Abstract: In recent years, the application of computer and artificial intelligence technology in the healthcare industry has become more and more common. With the rapid development of computational intelligence, medical imaging has realized the transformation from two-dimensional to four-dimensional. This article proposes a method to track the blood vessel movement of the elderly by using four-dimensional medical imaging technology on the problem of cardiovascular and cerebrovascular diseases in the elderly that are common in medical clinics. The aim is to accurately and robustly locate the specific position of the blood vessel from the medical image data to reduce the elderly's cardiovascular. The occurrence of various complications during surgery improves the treatment rate. This article first introduces the related knowledge of the four-dimensional medical imaging technology and the vascular movement of the elderly, and then carries out the reconstruction experiment of the four-dimensional model of blood and blood vessel wall, in order to further explore the effect of the four-dimensional medical imaging technology on the intravascular blood movement of the elderly patients with cardiovascular disease. To track and monitor the situation, this article again uses 200 patients with cardiovascular and cerebrovascular diseases admitted to our hospital from 2019 to 2020 as the experimental research objects, and took 50 volunteers who received health examinations in our hospital during the same year as experimental control subjects. Through the use of four-dimensional medical color ultrasound imaging technology to detect ECG and echocardiographic parameters of the two groups of patients, it was found that the ECG parameters of the experimental group were significantly greater than those of the control group, with significant statistical differences ($P<0.05$); The values of left ventricular systolic diameter and left ventricular end diastolic pressure in the electrocardiogram parameters of patients with coronary heart disease in the experimental group were significantly increased compared with the control group, while the ventricular ejection fraction and cardiac-to-mitral valve ratio were significantly decreased compared with the control group.

1. Introduction

1.1. Background and Significance

With the development of social econoour and the improvement of living standards, the aging of our country's population has become more and more serious, and various elderly cases of cardiovascular and cerebrovascular diseases such as coronary heart disease and cerebral hemorrhage are emerging one after another. As one of the vulnerable groups in society, the elderly, their health and living standards are a matter of great concern to the country and society. In order to reduce the probability of death of the elderly due to cardiovascular and cerebrovascular diseases, medical experts have been persistently exploring, hoping to achieve dynamic tracking of the vascular movement of the elderly in an effective way, so that elderly patients can be quickly and quickly detected Abnormal changes in blood vessels.

In recent years, with the rapid development of computer technology and the advancement of video imaging technology, computational intelligence is becoming more and more common in the field of healthcare, medical imaging has gradually moved towards digitization, realizing the functional transformation from two-dimensional to three-dimensional, and even today's four-dimensional, integrating the time factor into three-dimensional volume data. The formation of 3D+T four-dimensional medical imaging, which is widely used in clinical medicine. This article also proposes a four-dimensional medical imaging-based vascular motion tracking method for the elderly. According to the needs of human cardiovascular imaging, four-dimensional imaging can provide complete dynamic three-dimensional information of the heart structure, and more accurately reflect the range of motion of the chest cavity and abdomen. It can monitor and describe the trajectory of blood vessel movement throughout the heartbeat and respiratory cycle, and improve the accuracy and robustness of blood vessel movement tracking.

1.2. Related Work

For a long time, due to various cardiovascular and cerebrovascular diseases, the quality of life of many elderly people is low, and even the death rate caused by this is high every year. In order to reduce the pain and suffering of the elderly, improve the physical health of the elderly, and thereby improve the quality of life of the elderly, many medical experts are trying to conduct research and analysis on this aspect. Geng, Huan and Yang, Jinzhu et al. proposed an automatic 3D multi-scale pulmonary vessel segmentation method, in which the multi-label MRF optimization method is used for scale selection. First, in order to obtain morphological information of various blood vessels, the tubular characteristics of blood vessels are detected based on some eigenvalue analysis mechanism of Hessian matrix. Then, they introduced multi-label MRF optimization to correlate the scales of neighboring voxels. After applying the vascular enhancement filter, the whole blood vessel tree is segmented by the threshold method and the connectivity analysis method. Their research results show that the algorithm can not only distinguish other tissues, but also can successfully detect most blood vessels [1]. In addition, B Liu and B Liang used 4D visualization technology to rotate and collect X-ray blood vessels on the C-arm to make images to track and monitor the coronary arteries. They proposed and verified a method to visualize 4D arteries based on the propagation of 3D coronary images. They used nearest neighbor ECG gating to divide angiography into different cardiac stages, and then used motion-compensated iterative reconstruction methods to reconstruct high-quality 3D coronary artery images in one stage. Then, by registering the reconstructed image to the angiogram of each stage, it is propagated to other cardiac stages (I-stage registration). A third-order B-spline is used to model the vascular motion, and the parameters are solved by maximizing the normalized correlation (NC) between the 3D image projection and the angiogram

under the constraints of motion smoothness and volume preservation. Since the corresponding angiogram contains residual blood vessel motion, and the registration method can only match the average blood vessel morphology, there is still a morphological mismatch between the transmitted image and each angiogram. In order to obtain an accurate blood vessel morphology based on each angiogram, they further used the above-mentioned registration method (Phase II registration) to register the transmitted image to each angiogram. The final results show that their proposed method continuously spreads every 5% of the reconstructed images in the end-diastole (0%) to the end-systole (40%). After the first stage of registration, the average distance between the center line of the propagated true ground container and the center line of the ground true container was reduced from 2.2 ± 1.2 mm to 0.6 ± 0.2 mm. After phase II registration, the average centerline distance was further reduced to 0.5±0.2 mm [2]. In short, there are many researches on vascular diseases and motion trajectories in the elderly. This article only puts forward some shallow views and opinions on the basis of the research results of the predecessors, hoping to provide references and references for the clinical treatment of vascular diseases in the elderly.

1.3. Innovations in this Article

The innovations of this paper are mainly reflected in the following aspects: (1) Using the current advanced medical imaging technology, propose a method for tracking the vascular movement of the elderly based on four-dimensional medical imaging; (2) The acceleration of the aging process makes the society. There is a significant increase in the number of elderly diseases such as cardiovascular and cerebrovascular diseases, and the mortality rate of the population is also high. Based on this, this paper studies the vascular movement tracking method of the elderly with great social practical significance and reference value.

2. Method for Tracking Vascular Movement in the Elderly Based on Four-Dimensional Medical Imaging

2.1. Computational Intelligence and Medical Imaging Technology

(1) Computational intelligence

Computational intelligence is an important field of artificial intelligence. It has the characteristics of intelligence, parallelism, and robustness. It has good adaptive capabilities and strong global search capabilities, and has good computational effects in solving some complex problems. This intelligent computing method simulates the evolutionary process of nature, animal group behavior or human thinking language, etc. Its superior computing performance has attracted attention and recognition from all walks of life, and is widely used in optimized computing, pattern recognition, and biological medicine, electrical engineering and other fields.

(2) Overview of medical imaging

Medical imaging is also called medical imaging and medical imaging. It is a technology and processing process for obtaining images of human internal tissues in a non-invasive way for medical treatment or medical research on the human body. It usually involves two relatively independent research fields, including medical image systems and medical image processing [3-4].

(3) Medical imaging technology

Medical imaging is the fastest-growing subject in medicine. Its imaging technology has developed from simple X-rays to a variety of imaging technology applications, and its digitalization is also deepening, achieving from two-dimensional to three-dimensional. Even four-dimensional functional imaging transformation [5]. Common medical imaging techniques are as follows:

First, vascular photography. Also called arterial photography and angiography, it uses X-infrared

rays to irradiate the human body to observe the distribution and changes of blood vessels in the human body, including arterial blood vessels, venous blood vessels, and atrioventricular.

Second, cardiovascular imaging. It is mainly aimed at the treatment of cardiovascular diseases. The principle is to quickly inject the contrast agent into the thoracic cavity and blood vessels of the human heart through a cardiac catheter, so that the heart and blood vessels can be visualized under X-ray irradiation, and then the heart and blood vessels can be quickly developed through the instrument. Take it, and then analyze the changes in blood flow in the blood vessel and the changes in the heart and blood vessels based on the captured images.

Third, computer tomography. It is also called electronic computed tomography. According to the different scanning methods, there are X-ray scanning, Y-ray scanning and ultrasound.

Fourth, mammography. Mainly for the detection and treatment of women's breast diseases, it uses low-dose X-rays to examine women's breasts, which is conducive to early detection of breast tumors and cysts.

Fifth, positron emission tomography. Mainly used for clinical diagnosis and treatment of tumors. It is a nuclear medicine imaging technology that can provide three-dimensional dynamic images of the whole body. It can image the metabolism, functions and receptors of the human body in the way of image anatoour. It is non-invasive specialty.

Sixth, MRI. By drawing the internal structure of the human body in the form of electromagnetic waves.

Seventh, medical ultrasound examination. Ultrasound is what we usually call ultrasound. It uses its own physical characteristics to evaluate and judge the physical characteristics, morphological structure, and functional state of the human body. With the help of a computer system, the human muscle tissue and internal organs can reach visualization [6-7].

(4) Digital development of medical imaging and four-dimensional medical imaging

With the rapid development of electronic computer technology, a series of related technologies, disciplines, and sub-disciplines have developed rapidly, and achieved unprecedented outstanding results. Imaging technology is closely related to electronic computers. In recent years, its development momentum has been rapid. It has been widely used in all aspects, especially in medicine. Medical imaging, which combines imaging technology and medicine, is the fastest growing discipline in medicine. Its equipment and imaging quality are gradually moving towards digitalization. The most significant of these is the digitization of computer tomography and magnetic resonance imaging. The temporal and spatial resolution of these two imaging technologies have been greatly improved, and the basic two-dimensional realization of three-dimensional or even four-dimensional functional transformation, the diagnostic accuracy of images is greatly improved [8-9].

At present, the four-dimensional medical imaging technology is clinically used four-dimensional color ultrasound, also called four-dimensional medical color ultrasound imaging technology, which adds a fourth-dimensional time vector to the three-dimensional medical color ultrasound imaging. Four-dimensional medical ultrasound imaging technology can provide more abundant image information for clinical ultrasound diagnosis, reduce missed diagnosis of lesions, and effectively improve the quality of diagnosis. It is suitable for applications in multiple medical fields such as obstetrics and gynecology, cardiovascular and pediatrics [10].

2.2. Vascular Movement and Cardiovascular and Cerebrovascular Diseases

Vascular movement specifically refers to the flow of blood in blood vessels. It belongs to the research scope of hemodynamics. It is a science that studies blood deformation and flow. It mainly explores the effect of blood and plasma viscosity on the body, analyzes blood flow, blood flow

resistance and blood pressure and the relationship between them [11].

Cardio-cerebrovascular disease is a type of disease that often occurs in middle-aged and elderly people over the age of 50. It is a collective term for cardiovascular and cerebrovascular diseases. It is a type of heart caused by hyperlipidemia, atherosclerosis or hypertension. Ischemic or hemorrhagic diseases in the brain or body tissues. This disease has an extremely high prevalence, disability and fatality rate, posing a serious threat to the health of middle-aged and elderly people. The number of deaths due to cardiovascular and cerebrovascular diseases is as high as 15 million worldwide every year, and it has become a human death. The number one killer with the highest cause [12].

2.3. Four-Dimensional Color Doppler Ultrasound Imaging Technology Tracks and Predicts the Vascular Movement of the Elderly

Taking elderly patients with heart disease as experimental subjects, using four-dimensional color Doppler ultrasound imaging technology to track and explore changes in cardiovascular blood in elderly patients with heart disease through four-dimensional modeling.

After the four-dimensional original endocardium model is formed, the spatial processing of the data points and the momentum color gradient control complete the four-dimensional modeling of blood vessels. Then, according to the constructed three-dimensional model of the endocardium and epicardium, data points are obtained from each layer at the same angle as the center during the four-dimensional modeling process to generate endocardial and epicardial points. Since the rules are roughly the same, the calculation only needs to calculate the endocardial and epicardial points at the same time sequence, and this point is the myocardial thickness. Suppose there is a data point Q in the first time series, the coordinate in the inner membrane is $Q_1(x_1, y_1, z_1)$, and the coordinate in the outer mold is $Q_2(x_2, y_2, z_2)$; in the second time series, its corresponding point P, the inner membrane coordinate is $P_1(a_1, b_1, c_1)$, and the outer mold coordinate is $P_2(a_2, b_2, c_2)$. Then the ourocardial thickness vector at this point in the first-time sequence is:

$$|D_1|^2 = (x_2 - x_1)^2 + (y_2 - y_1)^2 + (z_2 - z_1)^2 \tag{1}$$

$$|D_2|^2 = (a_2 - a_1)^2 + (b_2 - b_1)^2 + (c_2 - c_1)^2 \tag{2}$$

The change in ourocardial thickness between the two points is $|D_2 - D_1|$.

3. Measurement of Hemodynamic Parameters Based on Four-Dimensional Vascular Reconstruction

In order to deeply explore the blood flow and movement rules in the blood vessels of the elderly, track and understand the abnormal conditions of the blood vessels of the elderly in time, and provide help for the prediction and diagnosis of the cardiovascular and cerebrovascular diseases of the elderly, this article uses four-dimensional medical imaging technology, the four-dimensional reconstruction of the blood model can achieve quantitative measurement of related hemodynamic parameters and observe the abnormal distribution of blood vessel walls due to blood flow and the periodic motion of the heart.

3.1. Three-Dimensional Reconstruction of Blood Vessels

To realize the transformation of the four-dimensional model, we must first build a

three-dimensional model of the blood vessel. For this reason, we introduce medical ultrasound imaging technology to realize the three-dimensional modeling of the blood vessel. The specific steps are as follows:

(1) Image acquisition and preprocessing

A pair of X-ray blood vessel contrast pictures are collected at the end of the catheter, and a series of intravascular ultrasound images are extracted and collected through a continuous ultrasound catheter. After filtering and denoising the original image, it is rendered to improve the visual clarity of the image. In the meantime, we used weighted average method and median filter method to filter and denoise the ultrasound image.

Assuming that the gray value of (x, y) point is $A(x, y)$, take a 3×3 template, and the reciprocal of the gradient is:

$$G(x, y : i, j) = \frac{1}{|A(x+i, y+j) - A(x, y)|} \tag{3}$$

The weight matrix formed by the reciprocal of gray scale samples is:

$$W = \begin{bmatrix} w(i-1.j-1) & w(i-1, j) & w(i-1, j+1) \\ w(i, j-1) & w(i, j) & w(i, j+1) \\ w(i+1, j-1) & w(i+1, j-1) & w(i+1, j+1) \end{bmatrix} \tag{4}$$

Among them, $w(i, j) = \frac{1}{2}$, the sum of other values is also $\frac{1}{2}$, then

$$w(x+i, y+j) = \frac{1}{2} \frac{G(x, y : i, j)}{\sum_i \sum_j G(x, y : i, j)} \tag{5}$$

After that, the median filter method is used to denoise the image. The principle is to use a sliding window of length m with an odd number of points, and replace the gray value of the center point pixel with the median value of the gray value of each point in the window Value, expressed by formula (4)

$$G_i = Med\{A_{i-e}, \ldots\ldots, A_{i+e}\} \tag{6}$$

Then use the dual-tree complex wavelet transform method to filter. The dual-tree complex wavelet is obtained on the basis of the complex wavelet, and a filter is added on the basis of one filter, so that the complex wavelet transform is in two filters. The one-dimensional data transformation formula is:

$$\psi(t) = \psi_h(t) + i\psi_g(t) \tag{7}$$

When the complex wavelet becomes a dual-tree complex wavelet, its two-dimensional data transformation formula is:

$$\psi(x, y) = \psi(x)\psi(y) \tag{8}$$

The dual-tree complex wavelet has better effect in decomposition and reconstruction, and is more conducive to the processing of image information details.

(2) Three-dimensional modeling of lumen axis and catheter retraction path

First, take out the lumbar spine from the front catheter and the back catheter of the angiographic image, and then use the compression method of the lumbar spine to align the projection point

between the two front images. Finally, the 3D model of the combined element space is calculated according to the geometric transformation between different angles.

(3) Extraction of inner and outer membrane contours

Segment the ultrasound images in blood vessels to extract the inner and outer membrane contours of the blood vessel wall.

(4) Determine the spatial orientation of intravascular ultrasound images in each frame

In intravascular ultrasound imaging, the catheter is located in the center of the image and usually does not coincide with the center of gravity of the lumen contour. The intersection of the axis of the lumen of the reconstructed blood vessel from the angiographic image and the plane of the intravascular ultrasound image also does not coincide with the center of gravity of the light profile in the image. Using the above two types of eccentricity information, by minimizing the weighted average of the eccentric angles between the axis intersections, the absolute azimuth angle of each frame of the intravascular ultrasound image and the ultrasound image plane and the light's center of gravity contour can be calculated.

3.2. Conversion and Realization of Four-Dimensional Vessel Modeling

After completing the three-dimensional reconstruction of the blood vessel, the next step is to perform a four-dimensional transformation of the model, where we need to set the initial conditions and boundary condition loads. The initial conditions are mainly to define the physical properties of blood vessels and blood, including the density, elasticity, Poisson's ratio of the materials used in blood vessel modeling, and the density, concentration and temperature of the simulated blood flow.

(1) Initial conditions

First, the selection of vascular material parameters. In this modeling experiment, common materials are selected as the model blood vessels. Since elastic materials are prone to iterations that do not converge during calculation, we do not consider the elasticity of blood vessels here. Let the blood vessel density be $\rho_1 = 1.007 g/cm^3$, the modulus be $E_p = 4e^5 Pa$, and the Poisson's ratio be $E_p = 4e^5 Pa$.

Second, the selection of blood material parameters. The specific blood material parameters of this experiment are shown in Table 1. Each parameter is the average value of the human body under normal physiological conditions. Since the fluid-solid coupling between the blood vessel wall and the blood in the modeling does not consider the effect of human body temperature, in this experiment we directly set the temperature parameter as the normal human body temperature of 37℃.

Table 1. Human blood parameter values

Blood densityρ(g/m³)	1.201	Blood viscosity $\mu(dyn\ s/cm^2)$	0.05	Cyclic period of pulsating flow $T(s)$	0.9
Valley average import speed $V_{min}(cm/s)$	8.1	Valley Reynolds number Re_{min}	145	Womersley number a	0.57
Peak average import speed $V_{max}(cm/s)$	56	Peak Reynolds number Re_{max}	946	Dean number D_n	413

(2) Boundary conditions

As a variable, the nerves and blood vessels in the human body are subject to certain restrictions. In other words, the freedom to enter the blood vessel outlet should be restricted, that is, in order to reduce the blood flow in the blood vessel, the entry and exit of the blood vessel should be controlled as a decision that should be fixedly controlled. On the outer wall surface of the blood vessel, there is

no need to set up barriers, as long as it remains free.

Regarding the fluid part, the boundary conditions for numerical blood flow simulation at the interface between the inlet and outlet of the blood flow are specified:

First, the blood flow rate in the blood vessel is controlled between 8.1cm/s-53.2cm/s;

Second, set the boundary conditions of the artery outlet, and set the outlet pressure to 0;

Third, set the inner wall surface of the blood vessel as the coupling surface of the blood and the blood vessel.

(3) Set load

The load of blood flow is the fluid velocity that mimics blood flow.

(4) Solution control

First, define the time step. The choice of time step is mainly related to the size of the device grid. The smaller the step of the dense grid time interval, the greater the possibility of final convergence.

Second, the control of solving equations. The start time of the input equation solution, the selection of the solution method, the convergence criterion and the control of the information error must be set in advance.

According to the above steps, four-dimensional modeling of blood vessels can be realized.

3.3. Control Equations of Blood Flow and Blood Vessel Wall Motion

(1) The control equation of blood flow

Since this experiment does not consider the influence of human body temperature, the influence of temperature is ignored during the coupling calculation of blood, and only the continuity equation and momentum conservation equation are established and the boundary conditions of the fluid are set. In the calculation, we use Navier-Stokes equation and continuous equation with zero velocity divergence to describe the fluid flow that mimics blood. The Navier-Stokes equation of blood fluid is:

$$\frac{\partial u}{\partial t} - \upsilon \nabla^2 u + u_g \nabla u + \frac{1}{\rho} \nabla p = f \tag{9}$$

Where ρ represents the density of blood, u represents the speed of blood flow, u_g represents the speed of grid points, μ represents the viscosity of blood, $\upsilon = \frac{\mu}{\rho}$ represents the coefficient of blood kinematic viscosity, P represents the pressure value of blood, and f represents the force.

The continuity equation of blood fluid is:

$$\nabla u = 0 \tag{10}$$

Set the boundary conditions of blood flow speed as:

$$\begin{cases} u\Big|_{interface} = \dfrac{\partial x}{\partial t} \\ \dfrac{\partial u}{\partial n}\Big|_{inlet} = 0 \\ \dfrac{\partial u}{\partial n}\Big|_{oulet} = 0 \end{cases} \tag{11}$$

Among them, the inlet represents the blood inlet, and the outlet represents the blood outlet.

Set the blood pressure boundary conditions as:

$$P\big|_{inlet} = P_{in}(t) \tag{12}$$

$$P\big|_{outlet} = P_{out}(t) \tag{13}$$

(2) Control equation of blood vessel wall motion

Suppose the motion equation of the blood vessel wall is:

$$\rho \frac{\partial^2 v_i}{\partial t^2} = \sum_{j=1}^{3} \frac{\partial \sigma_{ij}}{\partial x_j} + \rho_s f_i \tag{14}$$

Among them, $i, j = 1,2,\ldots\ldots,$ n , v_i represents the displacement coordinates of the blood vessel wall, σ_{ij} represents the stress tensor of the blood vessel wall, ρ_s represents the density of the blood vessel wall, and f_i represents the physical force acting on the solid part of the blood vessel wall, x_j represents the direction along the four coordinate axes in the four-dimensional coordinate system.

The strain displacement relationship of the blood vessel wall is:

$$\varepsilon_{ij} = \frac{1}{2}\left(\frac{\partial v_i}{\partial x_j} + \frac{\partial v_j}{\partial x_j}\right) \tag{15}$$

Among them, $i, j = 1,2,\ldots\ldots,$ n , ε_{ij} represents the strain tensor of the blood vessel wall, and v represents the displacement coordinate of the blood vessel wall.

Set the outer surface of the blood vessel wall as a free surface:

$$\sigma_{ij} n_j\big|_{outwall} = 0 \tag{16}$$

Outwall represents the outer wall surface of the blood vessel wall.

(3) Coupling boundary control of blood and blood vessels

The coupling surface between blood and blood vessel is the contact surface between blood and blood vessel, that is, the inner surface of the blood vessel wall. In order to ensure the effective monitoring of the blood flow law, we need to set the coupling condition on the inner surface of the blood vessel wall, as in equation (17)

$$\sigma_{ij}^{f} n_j\Big|_{\text{interface}} = \sigma_{ij}^{w} n\Big|_{\text{interface}} \tag{17}$$

Among them, interface represents the inner surface of the blood vessel wall, σ_{ij}^{f} represents the stress tensor of blood, and σ_{ij}^{w} represents the stress tensor of the blood vessel wall.

3.4. Calculation and Processing of Experimental Results and Data

The data processing of this experiment uses a modified version of ANSYS, which displays the voltage distribution on the blood vessel wall in color, and graphically represents the instantaneous smooth changes. This method not only improves the recognition ability and efficiency of numerical simulation, but also provides a more intuitive display of complex calculation results and realizes the visualization of calculation results.

4. Analysis of the Tracking Results of Elderly Blood Vessel Movement Based on Four-Dimensional Medical Images

In the third part of this article, a four-dimensional vascular model is constructed. Now for further research and analysis of the results of four-dimensional medical image tracking and monitoring of the vascular movement of the elderly, in this chapter we will take the 200 cases of heart and brain admitted to our hospital from 2019 to 2020 patients with vascular diseases are the research subjects (including hypertension patients, coronary heart disease patients, angina patients, cerebral thrombosis patients, and acute myocardial infarction patients). To explore the tracking and monitoring of intravascular blood flow in these patients by four-dimensional medical color ultrasound imaging technology.

According to the different types of patients, these 200 patients were divided into hypertension group (A), coronary heart disease group (B), angina pectoris group (C), cerebral thrombosis group (D), and acute myocardial infarction group (E). The above are all listed as the experimental group. In addition, 50 volunteers who have undergone physical examinations in our hospital from 2019 to 2020 are selected as the experimental control group. After examination, these 50 volunteers have no medical history and are in good physical condition. Among them, 30 are male and 20 are females, aged 46-78 years old, with an average age of 51.2±7.45 years old. In the experimental group, there were 34 cases in group A, including 18 males and 16 females, with an average age of 64.23±6.75 years and an average age of 13±2.4 years; there were 37 cases in group B, including 20 males and 17 females, with an average The age was 61.22±5.62 years old, with an average age of 10±3.5 years; there were 41 cases in group C, including 23 males and 18 females, with an average age of 65.73±3.71 years old and an average age of 9±3.7 years; there were 38 cases in group D. Among them, there were 18 males and 20 females, with an average age of 68.16±3.45 years and an average age of 14±5.4 years; there were 50 cases in group E, including 27 males and 23 females, with an average age of 66.74±5.25 years and an average age of 11 ±3.4 years.

Before the experiment, explain the purpose of the experiment to all the patients participating in the test to obtain the patient's consent. After that, four-dimensional medical color ultrasound imaging technology was used to collect electrocardiograms and echocardiogram images of all patients participating in the experiment. Finally, all experimental data were collected, and SPSS22.0 statistical analysis software was used to analyze and process the experimental data. $P<0.05$ is regarded as a statistical difference between the groups.

4.1. Basic Situation Comparison between the Experimental Group and the Control Group

(1) Comparison of general conditions of patients

All patients who participated in this experiment were statistically data between age, gender, and age of illness to compare the differences between the two groups. The results of the comparison are shown in Table 2 and Figure 1.

Table 2. Comparison of general conditions of patients

Group	N	Men /Women	Average age	Sick age(year)
Group A	34	18/16	64.23±6.75	13±2.4
Group B	37	20/17	61.22±5.62	10±3.5
Group C	41	23/18	65.73±3.71	9±3.7
Group D	38	18/20	68.16±3.45	14±5.4
Group E	50	27/23	66.74±5.25	11±3.4
Control group	50	30/20	51.2±7.45	/

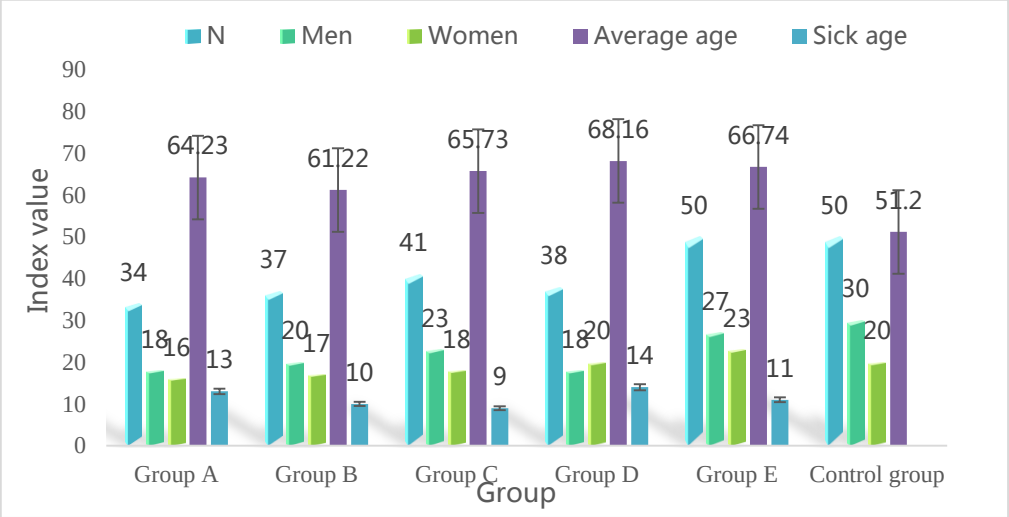

Figure 1.Comparison of general conditions of patients

According to Table 2 and Figure 1, after comparison and observation, the differences between the experimental group and the control group in the age, gender, age of disease and their disease types are small, and there is no statistical difference (P>0.05).

(2) Comparison of patient's heart rate, systolic blood pressure and diastolic blood pressure

Collect and record the heart rate, systolic blood pressure and diastolic blood pressure of the two groups of patients, and compare the differences between the two groups. The results are shown in Table 3 and Figure 2.

Table 3. Comparison of patient's heart rate, systolic and diastolic blood pressure

Group	N	Systolic blood pressure (mmHg)	Diastolic blood pressure (mmHg)
Group A	34	134.15±13.01	81.42±11.30
Group B	37	135.23±12.05	82.12±10.20
Group C	41	137.12±11.81	83.42±11.17
Group D	38	132.45±12.62	81.32±11.34
Group E	50	136.35±15.21	82.36±10.32
Control group	50	132.60±13.14	79.47±13.06

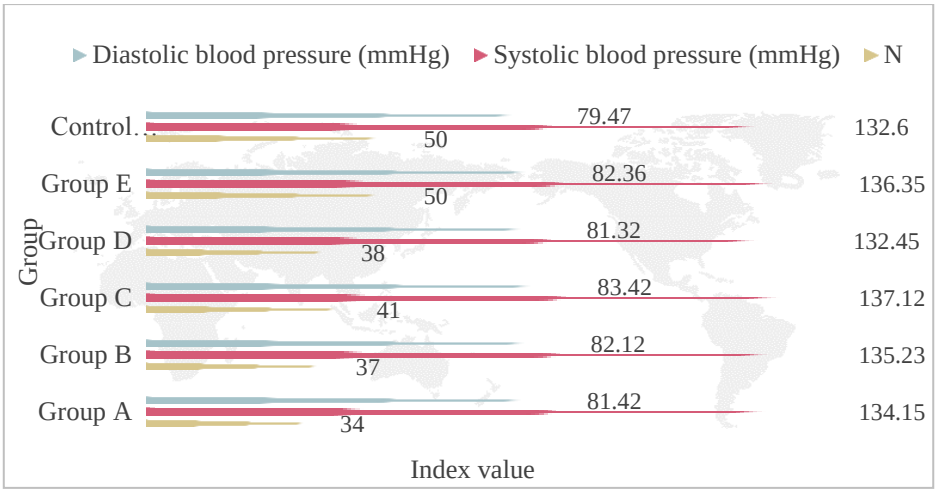

Figure 2.Comparison of patient's heart rate, systolic and diastolic blood pressure

According to Table 3 and Figure 2, after comparison and observation, the differences in heart rate, systolic blood pressure, and diastolic blood pressure between the experimental group and the control group were small, and there was no statistical difference (P>0.05).

4.2. Comparison of ECG Parameters between Experimental Group and Control Group

In the experiment, ECG was collected on the two groups of patients, and the magnetic resonance imaging (QRS) time limit, QT interval extension, QTC interval extension, ST segment, T wave and R wave related indicators were detected and recorded. The specific conditions are shown in Table 4 and Figures 3 and 4.

Table 4. Comparison of patient ECG parameters

Group	QRS time limit extension (ms)	QT interval prolongation (≥400ms, ms)	QTC interval prolongation (ms)	ST depression (≥0.6mv)				Poor R wave increment
				Front wall	Anterolateral	Lower wall	High sidewall	
Group A(n=34)	25(12.5%)	24(12%)	26(13%)	23(11.5%)	30(15%)	26(13%)	21(10.5%)	22(11%)
Group B(n=37)	31(15.5%)	30(15%)	25(12.5%)	24(12%)	23(11.5%)	28(14%)	24(12%)	30(15%)
Group C(n=41)	35(17.5%)	32(16%)	36(18%)	37(18.5%)	25(12.5%)	36(18%)	35(17.5%)	37(18.5%)
Group D(n=38)	32(16%)	35(17.5%)	33(16.5%)	34(17%)	35(17.5%)	34(17%)	27(13.5%)	34(17%)
Group E(n=50)	47(23.5%)	36(18%)	42(21%)	41(20.5%)	35(17.5%)	39(19.5%)	45(22.5%)	46(23%)
Control group(n=50)	5(2.5%)	4(2%)	2(1%)	7(3.5%)	3(1.5%)	4(2%)	2(1%)	8(4%)

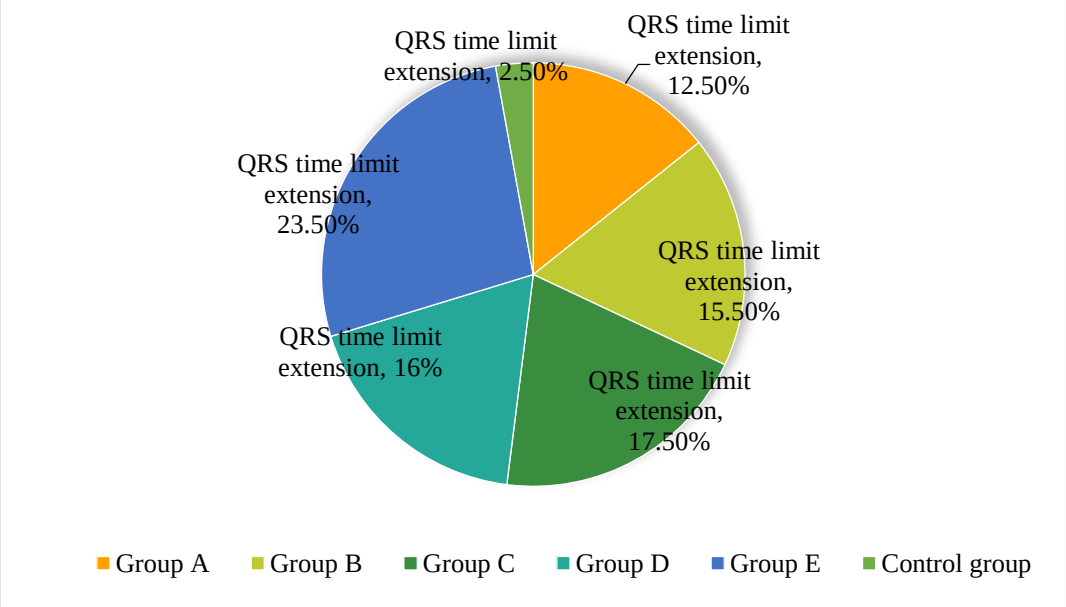

Figure 3.Comparison of patient ECG parameters

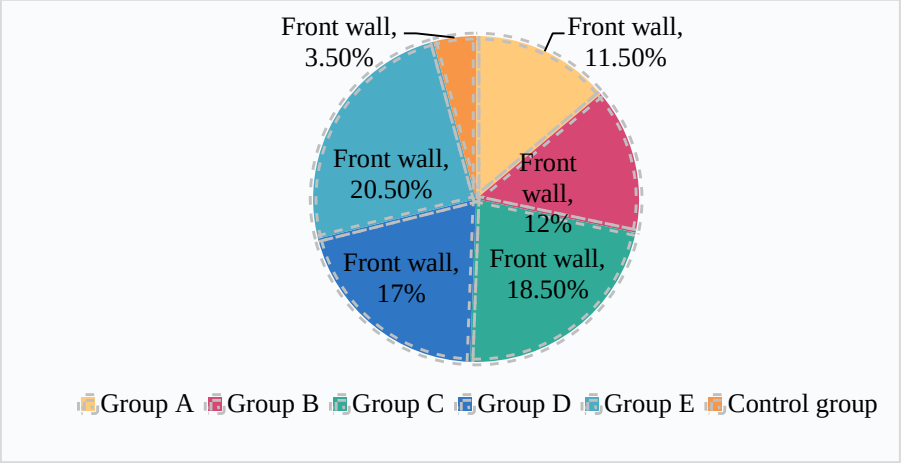

Figure 4. Comparison of the index values of the two groups in the ST segment

It can be seen from Table 4, Figure 3 and Figure 4 that the experimental group experienced prolonged QRS time limit, prolonged QT interval, prolonged QTC interval, anterior partition, anterior wall, anterior wall, inferior wall and high sidewall ST segment depression the number of patients with low or inverted T waves and poor R wave progression was significantly more than the control group. Among them, the three groups C, D, and E accounted for the largest proportion, accounting for 18.5%, 17% and 20.5% respectively; the parameters of the group electrocardiogram are relatively small, and the largest number of people is the presence of low ST depression or T wave flat or inverted anterior wall, accounting for 3.5%. After calculating the $P<0.05$ between the two groups, the difference of ECG parameters between the two groups was statistically significant.

4.3. Comparison of Echocardiographic Parameters between the Experimental Group and the Control Group

The two groups of patients were tested for conventional echocardiographic parameters. Left ventricular end diastolic pressure (LVEDD), left ventricular intrasystolic diameter (LVEDS), left ventricular ejection fraction (LVEF), and cardiac mitral valve ratio (E/ A), the measurement result is shown in Table 5 and Figure 5.

Table 5. Comparison of echocardiographic parameters between the two groups

	LVEDS	LVEDD	LVEF	E/A
Group A	50.13	58.46	41.23	0.98
Group B	51.36	57.14	39.57	0.87
Group C	49.25	57.49	42.16	0.95
Group D	52.14	57.16	40.27	0.78
Group E	48.55	54.36	39.88	0.85
Control group	29.34	42.79	63.47	1.79

According to Table 5 and Figure 5, in the experimental group, the left ventricular systolic diameter of group D was the largest at 52.14, followed by group B at 51.36, and the left ventricular end diastolic pressure of group A was the largest at 58.46; on the contrary, the left ventricular end diastolic pressure of group A was 58.46. The two index values are 29.34 and 42.79, respectively, and the two groups are significantly larger than the experimental group. In the experimental group,

the left ventricular ejection fraction was the highest in the C group, which was 42.16, and the cardiac-to-mitral valve ratio in the A group was the largest, which was 0.98. The control group was 63.47 and 1.79, respectively. Compared with the experimental group, the two groups were significantly reduced. Therefore, the differences in the parameters of echocardiography between the two groups were statistically significant (P<0.05).

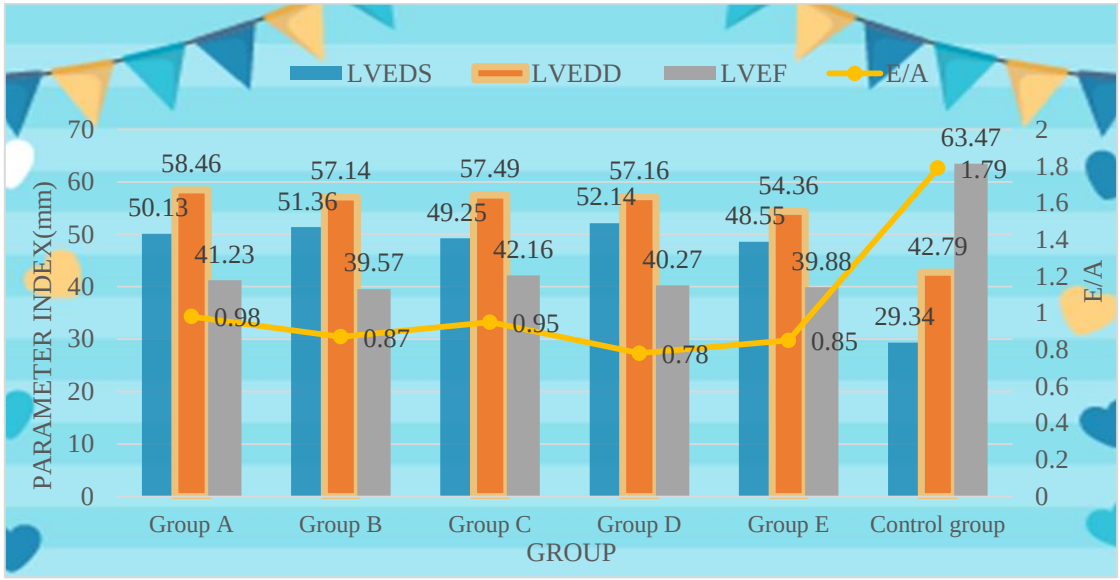

Figure 5. Comparison of echocardiographic parameters between the experimental group and the control group

4.1 Comparison of Echocardiographic Parameters between QRS Time Limit Normal Group and QRS Time Limit Extended Group

Compare the QRS time limit of the experimental group within the same group, and compare the difference in the conventional echocardiogram parameters of patients with normal QRS time limit and extended QRS time limit in the experimental group. Among them, the number of patients with normal QRS time limit is 117, and the QRS time limit is extended. The number of patients was 83, and the results are shown in Table 6 and Figure 6.

Table 6. Comparison of echocardiographic parameters between QRS time limit normal group and QRS time limit extended group

	LVEDS	LVEDD	LVEF	E/A
QRS time limit normal group	48	53	46	4
QRS time limit extension group	47	59	39	4

It can be seen from Table 6 and Figure 6 that compared with the normal QRS time limit group, patients in the QRS time limit extended group had significantly increased LVEDD and a significantly lower LVEF. The difference between the two groups was large and statistically significant (P<0.05); but the difference in LVEDS and E/A between QRS time limit normal group and QRS time limit extended group was small, and there was no statistical difference between the two (P>0.05).

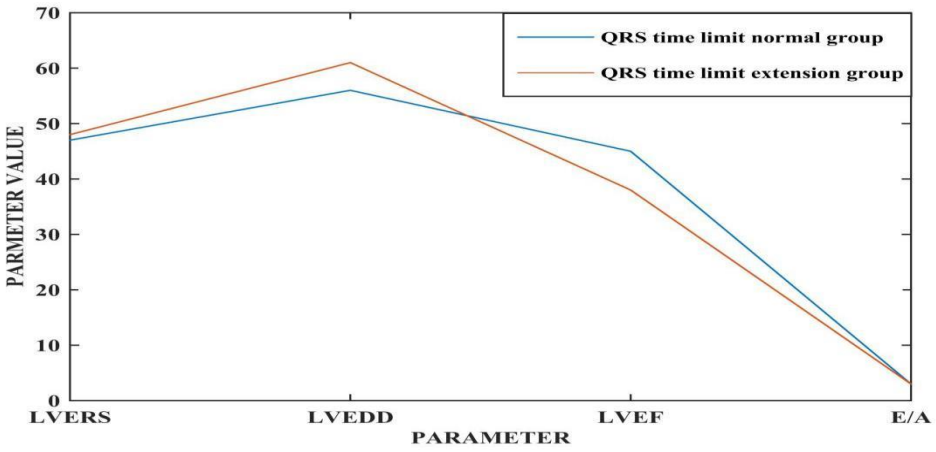

Figure 6. Comparison of echocardiographic parameters between QRS time limit no

4.2 Comparison of Four-Dimensional Strain of Echocardiographic Systolic Parameters between QRS Time Limit Normal Group and QRS Time Limit Extended Group

The four-dimensional strain changes of the apical, middle, basal, and left ventricle in the QRS normal group and QRS extended group during echocardiographic systole were measured, and the differences in various indicators between the two groups were compared. The results are shown in Table 7 and Figure 7.

Table 7.Comparison of four-dimensional strain of echocardiographic systolic parameters between QRS time limit normal group and QRS time limit extended group

	Apical segment	Middle section	Basal segment	Four-dimensional strain
QRS time limit normal group	15.5	15	12.5	18
QRS time limit extension group	10	10	11	14

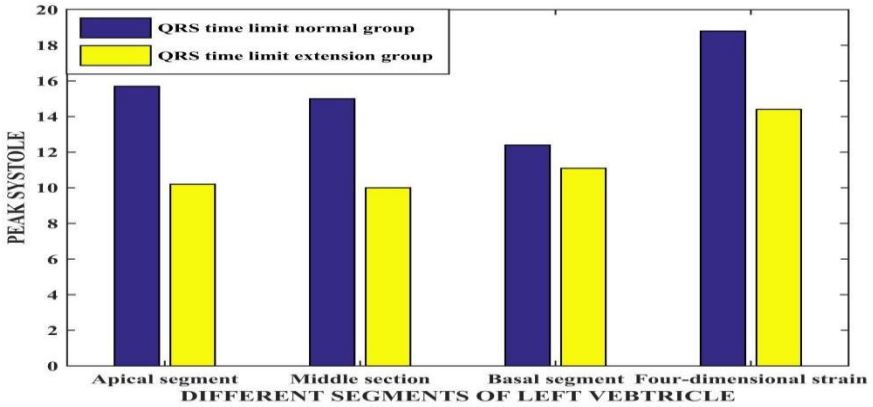

Figure 7. Comparison of four-dimensional strain of echocardiographic systolic parameters between QRS time limit normal group and QRS time limit extended group

It can be seen from Table 7 and Figure 7 that compared with the QRS time limit normal group, the QRS time limit extended group has significantly lower four-dimensional strain values in the apical, middle, basal and left ventricle during the echocardiographic systole. The difference is large

and statistically significant (P<0.05).

5. Conclusions

Since entering the 21st century, our country has gradually entered an aging society and has become an elderly country. At present, our country is the country with the largest elderly population in the world, and the huge number of elderly populations makes our country's cardiovascular disease patients occupy a large proportion in the world. Cardiovascular disease is a type of ischemic or hemorrhagic disease that is common in middle-aged and elderly people. Its morbidity, disability and fatality rate are extremely high, which seriously threatens the health of the elderly.

With the development of science and technology and its application in medicine, medical imaging technology has developed rapidly in recent years. Following two-dimensional and three-dimensional, four-dimensional medical imaging technology has emerged and has gradually been applied in clinical diagnosis and treatment. Common four-dimensional medical imaging technology is four-dimensional medical color ultrasound imaging technology, which is mainly used for the detection and treatment of related diseases in obstetrics and gynecology, cardiovascular and pediatrics.

This study takes 200 patients with cardiovascular and cerebrovascular diseases treated in our hospital from 2019 to 2020 as the experimental research objects, and 50 volunteers who underwent physical examinations in our hospital in the same year were selected as the experimental control group. By using four-dimensional medical color ultrasound imaging technology was used to detect ECG parameters and echocardiogram parameters. The results found that the basic physical conditions of the two groups of patients, including age, gender, sick age, heart rate, systolic blood pressure, and diastolic blood pressure, were not statistically significant. In the experimental group, QRS time limit prolonged, QT interval prolonged, QTc interval prolonged, ST segment depression of the anterior septum, anterior wall, anterior wall, inferior wall and high side wall, low T wave flat or inverted, and poor R wave progression. The number of patients with other conditions was significantly more than that of the control group; the left ventricular systolic diameter and left ventricular end diastolic pressure in the ECG parameters of the experimental group of coronary heart disease patients were significantly increased compared with the control group, while the ventricular ejection fraction and cardiac cusp ratio was significantly reduced compared with the control group.

Funding

This article is not supported by any foundation.

Data Availability

Data sharing is not applicable to this article as no new data were created or analysed in this study.

Conflict of Interest

The author states that this article has no conflict of interest.

References

[1]Geng, H., Yang, J., Tan, W., & Zhao, D. (2016). "3d Multi-Scale Pulmonary Vascular

Segmentation Algorithm Based on Multi-Label Mrf Optimization". Journal of Medical Imaging and Health Informatics, 6(7), pp.1794-1798. https://doi.org/10.1166/jmihi.2016.1892

[2]Liu, B., Liang, B., Xu, X., Guo, B., & Wu, Q. (2016). "Tu-h-Campus-Iep2-02: Four-Dimensional Coronary Artery Visualization Based on Image Propagation". Medical Physics,43(6), pp.3780-3781. https://doi.org/10.1118/1.4957680

[3]Ballarin, F., Faggiano, E., Ippolito, S., Manzoni, A., Quarteroni, A., & Rozza, G., et al. (2016). "Fast Simulations of Patient-Specific Haemodynamics of Coronary Artery Bypass Grafts Based on a Pod–Galerkin Method and a Vascular Shape Parametrization". Journal of Computational Physics, 315(C), pp.609-628. https://doi.org/10.1016/j.jcp.2016.03.065

[4]Liu, T., Sun, M., Liu, Y., Hu, D., Ma, Y., & Ma, L., et al. (2019). "Admm Based Low-Rank and Sparse Matrix Recovery Method for Sparse Photoacoustic Microscopy". Biomedical Signal Processing & Control,52(JUL.), pp.14-22. https://doi.org/10.1016/j.bspc.2019.03.007

[5]Shimohigashi, Y., Araki, F., Toya, R., Maruyama, M., & Nakaguchi, Y. (2016). "Su-g-Jep4-06: Evaluation of Interfractional and Intrafractional Tumor Motion in Stereotactic Liver Radiotherapy, Based on Four-Dimensional Cone-Beam Computed Tomography Using Fiducial Markers". Medical Physics, 43(6), pp.3682-3682. https://doi.org/10.1118/1.4957116

[6]Appel, A. A., Larson, J. C., Jiang, B., Zhong, Z., Anastasio, M. A., & Brey, E. M. (2016). "X-Ray Phase Contrast Allows Three Dimensional, Quantitative Imaging of Hydrogel Implants". Annals of Biomedical Engineering, 44(3), pp.773-781. https://doi.org/10.1007/s10439-015-1482-5

[7]Li, Z., & Wang, Y. J. (2018). "A Health Informatics Study Based on Prognostic Value of Extravascular Lung Water Index Monitoring by Minimally Invasive Quantitative Measurement in Elderly Patients with Septic Shock". Journal of Medical Imaging & Health Informatics, 8(2),pp. 337-343. https://doi.org/10.1166/jmihi.2018.2306

[8]Zeina AR, Nakar H, Reindorp DN, Nachtigal A, Krausz MM, & Itamar I, etc. (2017). "Four-Dimensional Computed Tomography (4dct) for Preoperative Localization of Parathyroid Adenomas". Israel Medical Association Journal, 19(4), pp.216 -220.

[9]Morrison, J., & Kaufman, J. (2016). "Vascular Access Tracking System: a Web-Based Clinical Tracking Tool for Identifying Catheter Related Blood Stream Infections in Interventional Radiology Placed Central Venous Catheters". Journal of Digital Imaging, 29(6), pp.1-5.

[10]Zhao, F., Liang, J., Chen, X., Liu, J., Chen, D., & Yang, X., et al. (2016). "Quantitative Analysis of Vascular Parameters for Micro-Ct Imaging of Vascular Networks with Multi-Resolution". Medical & Biological Engineering & Computing, 54(2-3), pp.511-524. https://doi.org/10.1007/s11517-015-1337-0

[11]Chang Xiaoni, Xie Yan, Shen Yamei, Qiu Yingwu, & Ruan Litao. (2018). "The Application of Superb Micro-Vascular Imaging in Evaluating the Stability of Carotid Atherosclerotic Plaques and its Predictive Value for Stroke". Shaanxi Medical Journal, 047(012) , pp.1532-1535.

[12]Wang Lin, & Shen Guangshu. (2018). "Analysis of Intracranial Vascular Characteristics of Cerebral Infarction Patients with Low and High Risk According to the Essen Stroke Risk Score by 3d-Tof-Mra". Chinese Journal of Clinical Medical Imaging, 029(007),pp. 461 -463,467.